

FAR-FIELD RECONSTRUCTION FROM BI-POLAR DATA: AN EFFECTIVE MODELLING OF THE AUT

F.D'Agostino ⁽¹⁾, F.Ferrara ⁽¹⁾, C.Gennarelli ⁽¹⁾, R.Guerriero ⁽¹⁾, G.Riccio ⁽¹⁾, C.Rizzo ⁽²⁾

⁽¹⁾ *D.I.I.I.E. - University of Salerno, via Ponte Don Melillo, 84084 Fisciano (SA), Italy.
Email: gennar@diie.unisa.it*

⁽²⁾ *M.I.-Technologies (Europe) - 3 Hither Green Southbourne Emsworth, PO10 8JA, UK.
Email: crizzo@mi-technologies.com*

Abstract

A sampling interpolation algorithm for reconstructing the antenna far field from voltage data acquired via a bi-polar scanning in the near-field region is developed in this work. It makes use of a very flexible modelling of the source, which fits very well a lot of actual antennas. Numerical examples assessing the efficiency and the stability of the algorithm are presented. Such a reconstruction process allows one to get an efficient probe compensated near-field-far-field transformation with bi-polar scanning, which requires a number of data remarkably lower than that needed by the standard approach.

Introduction

As well-known, the evaluation of antenna far field (FF) from near-field (NF) measurements allows one to overcome those drawbacks which, for electrically large antennas, make unpractical to measure antenna patterns on a conventional FF range. Among the NF-FF transformation techniques, that employing the bi-polar scanning [1, 2] is particularly interesting. In such a scanning the antenna under test (AUT) rotates axially, whereas the probe is attached to the end of an arm which rotates around an axis parallel to the AUT one (see Fig. 1). This allows the collection of the NF data on a grid consisting of concentric rings and radial arcs. The bi-polar scanning maintains all the advantages of the plane-polar one [3], while providing a simple and cost-effective measurement system. In fact, since the arm is fixed at only one point and the probe is attached at its end, the bending is constant and this allows to maintain the planarity. Unfortunately, the original approach in [1] does not take advantage of the nonredundant representations of electromagnetic (EM) fields [4] and, as a consequence, it requires a useless large amount of NF data. This drawback has been overcome in [2] by using an ellipsoidal modelling of the source, which is particularly tailored to quasi-planar antennas. Aim of this paper is to develop an efficient probe-compensated NF-FF transformation with bi-polar scanning using an even more flexible source modelling, which fits very well a lot of actual antennas. Thus, a new sampling technique is developed to recover the data, required by the classical NF-FF with plane-rectangular scanning [5], from the knowledge of the bi-polar ones. It must be stressed that the proposed NF-FF transformation technique retains the numerical efficiency of the previous ones, while using a number of data remarkably lower than that needed by the original approach [1].

Voltage reconstruction over a plane from bi-polar samples

Let us consider an antenna enclosed in a convex domain bounded by a surface Σ with rotational symmetry and a non directive probe scanning a plane located in the NF region. For such a probe, the output voltage has the same effective spatial bandwidth of the field radiated by the AUT [2]. Since the plane can be described by radial lines and rings, in the following we deal with the voltage representation on an observation curve C characterized by an analytical parameterization $\mathbf{r} = \mathbf{r}(\xi)$. According to [4], let us introduce the "reduced voltage" $\tilde{V}(\xi) = V(\xi) e^{j\gamma(\xi)}$, where $V(\xi)$ is the measured probe voltage, $\gamma(\xi)$ is a proper phase function and ξ is an optimal parameter used to describe the observation curve on the plane. The bandlimitation error, occurring when the reduced voltage is approximated by a spatially bandlimited function, becomes negligible as the bandwidth exceeds a critical value W_ξ [4]. Therefore such an error can be effectively controlled by choosing a bandwidth equal to $\chi' W_\xi$, χ' being an excess bandwidth factor slightly greater than unity for an electrically large AUT.

When C is a radial line, by denoting with $s'_{1,2}$ the arclength coordinates of the two tangency points $P_{1,2}$ over C' (intersection curve between the meridian plane passing through the observation point P and Σ), with $R_{1,2}$ the distances from P to $P_{1,2}$ and choosing $W_\xi = \beta \ell' / 2\pi$ (ℓ' being the length of C'), we have [4]:

$$\gamma = (\beta/2) [R_1 + R_2 + s'_1 - s'_2] ; \quad \xi = (\pi/\ell') [R_1 - R_2 + s'_1 + s'_2] \quad (1)$$

When the observation curve is a ring, the phase function is constant and it is convenient to use the azimuthal angle φ as parameter. The corresponding bandwidth for a circle of radius ρ and center $(0,0,z)$ is [4]:

$$W_\varphi = W_\varphi(\rho, z) = \frac{\beta}{2} \max_z \left(\sqrt{(z-z')^2 + (\rho + \rho'(z'))^2} - \sqrt{(z-z')^2 + (\rho - \rho'(z'))^2} \right) \quad (2)$$

where $\rho'(z')$ is the equation of Σ in cylindrical coordinates.

In order to get a nonredundant representation, it is necessary to choose Σ with a regular surface fitting the AUT geometry. To this end, let us consider a surface Σ formed by two circular "bowls" with the same aperture diameter (equal to $2a$), arranged as shown in Fig. 2. Note that their lateral surfaces have not the same bend because they are generally determined by rotating two different circular arcs, each equal to a quarter of circumference, with radius c and c' , respectively. Accordingly, for this source modelling, the length of C' is:

$$\ell' = 2[(a-c) + (a-c') + (c+c')\pi/2] \quad (3)$$

Such a kind of surface allows to fit very well a lot of real antennas by properly choosing the values of three parameters, namely c , c' and a . By taking into account such a source modelling, the evaluation of γ and ξ for a radial line in Eq. 1, furnishes two different expressions depending on the range of the radial distance $\rho(\xi)$ (see Fig. 2). In fact, for $\rho < a$ the tangency points $P_{1,2}$ are both located on the upper bowl, whereas, for $\rho > a$, P_2 is on the lower one. Accordingly, if $\rho \leq a$, we get:

$$R_1 = \sqrt{(\rho+b)^2 + d^2 - c^2}; \quad s'_1 = -(b+c\alpha_1); \quad \alpha_1 = \tan^{-1}(R_1/c) - \tan^{-1}[(\rho+b)/d]; \quad b = a-c \quad (4)$$

$$R_2 = \sqrt{(b-\rho)^2 + d^2 - c^2}; \quad s'_2 = b+c\alpha_2; \quad \alpha_2 = \tan^{-1}(R_2/c) - \tan^{-1}[(b-\rho)/d] \quad (5)$$

and, if $\rho \geq a$, the expressions of R_1 , s'_1 and α_1 are again given by (4), whereas it results:

$$R_2 = \sqrt{(\rho-b')^2 + d^2 - c'^2}; \quad s'_2 = b+c\pi/2 + c'\alpha_2; \quad \alpha_2 = \tan^{-1}(R_2/c') - \pi/2 + \tan^{-1}[(\rho-b')/d]; \quad b' = a-c' \quad (6)$$

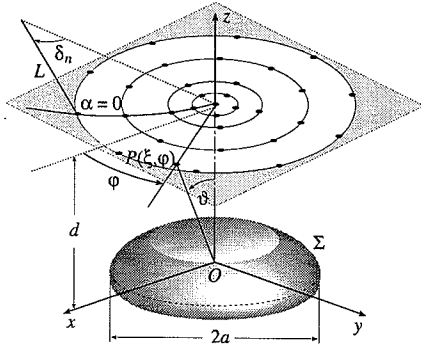


Fig. 1 - By-polar scanning.

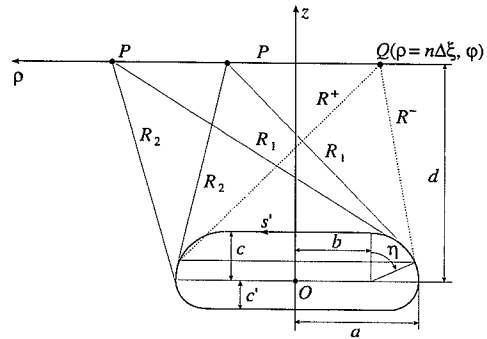


Fig. 2 - Geometry of the source modelling.

In the case of an azimuthal circumference of radius ρ and center $(0,0,d)$ the bandwidth (Eq. 2) corresponding to the parameter φ is explicitly given by:

$$W_\varphi = W_\varphi(\rho, z) = \frac{\beta}{2} \max_{0 \leq z' \leq c} \left(\sqrt{(d-z')^2 + (\rho + \rho'(z'))^2} - \sqrt{(d-z')^2 + (\rho - \rho'(z'))^2} \right) \quad (7)$$

To determine this maximum, it is convenient to introduce the angular coordinate η (see Fig. 2) such that $z' = c \cos \eta$ and $\rho'(z') = b + c \sin \eta$. Then, the sought maximum corresponds to the solution of the equation:

$$bd(\cos^2 \eta - \sin^2 \eta) + [\rho^2 + d^2 - b^2] \sin \eta \cos \eta - c(b \cos \eta + d \sin \eta) = 0 \quad (8)$$

which lies in the range $[0, \pi/2]$.

A point on the plane in the NF region can be specified by the bi-polar coordinate system using the AUT angle α , the angle δ and the length L of the arm. The standard polar coordinates are related to them by:

$$\rho = 2L \sin(\delta/2); \quad \varphi = \alpha - \delta/2 \quad (9)$$

A convenient way to obtain a nonredundant representation on a plane from bi-polar samples is to describe this last by means of radial lines and rings, as in the plane-polar case. The way of collecting the data in a bi-polar facility implies that the starting sample at $\alpha = 0$ on the n -th ring is shifted by $\varphi_0(\xi_n) = -\delta_n/2$ with respect to the corresponding one in the plane-polar scanning. As a consequence, the reduced voltage at any point on the plane can be reconstructed from the bi-polar data via the optimal sampling interpolation (OSI) formula:

$$\tilde{V}(\xi, \varphi) = \sum_{n=n_0-q+1}^{n_0+q} \left\{ \Omega_N(\xi - \xi_n) D_{N''}(\xi - \xi_n) \sum_{m=m_0-p+1}^{m_0+p} \tilde{V}(\xi_n, \varphi_{m,n}) \Omega_{M_n}(\varphi - \varphi_{m,n}) D_{M_n''}(\varphi - \varphi_{m,n}) \right\} \quad (10)$$

where $n_0 = \text{Int}(\xi / \Delta\xi)$, $m_0 = \text{Int}((\varphi - \varphi_0(\xi_n)) / \Delta\varphi_n)$ are the indexes of the sample nearest on the left to the output point, $2q, 2p$ are the number of retained samples along ξ and φ , and

$$\xi_n = n\Delta\xi = 2n\pi / (2N'' + 1); \quad \varphi_{m,n} = \varphi_0(\xi_n) + m\Delta\varphi_n = \varphi_0(\xi_n) + 2m\pi / (2M_n'' + 1) \quad (11)$$

$$N'' = \text{Int}(\chi N') + 1; \quad N' = \text{Int}(\chi' W_\xi) + 1; \quad N = N'' - N'; \quad M_n'' = \text{Int}(\chi M_n') + 1 \quad (12)$$

$$M_n' = \text{Int}(\chi^* W_{\varphi_n}) + 1; \quad M_n = M_n'' - M_n'; \quad \chi^* = \chi^*(\xi_n) = 1 + (\chi' - 1) [W_\varphi(\xi_n) / \beta a]^{-2/3} \quad (13)$$

$\chi > 1$ being the oversampling factor, needed to control the truncation error. Moreover,

$$D_{M''}(x) = \frac{\sin[(2M''+1)x/2]}{(2M''+1)\sin(x/2)}; \quad \Omega_M(x) = \frac{T_M \left[2(\cos(x/2)/\cos(x_0/2))^2 - 1 \right]}{T_M \left[2/\cos^2(x_0/2) - 1 \right]} \quad (14)$$

are the Dirichlet and Tschebyscheff Sampling (TS) functions [4], respectively, wherein $T_M(\cdot)$ is the Tschebyscheff polynomial of degree M . In (14) x_0 is equal to $q\Delta\xi$ or $p\Delta\varphi_n$.

Probe compensated NF–FF transformation and numerical results

The basic theory of probe compensated NF measurements on a plane as proposed in [5] is based on the application of the Lorentz reciprocity theorem. The key relations in the here used reference system are:

$$E_\vartheta(\vartheta, \varphi) = \left(I_H E'_{\varphi_V}(\vartheta, -\varphi) - I_V E'_{\varphi_H}(\vartheta, -\varphi) \right) / \Delta; \quad E_\varphi(\vartheta, \varphi) = \left(I_H E'_{\vartheta_V}(\vartheta, -\varphi) - I_V E'_{\vartheta_H}(\vartheta, -\varphi) \right) / \Delta \quad (15)$$

where $\Delta = E'_{\vartheta_H}(\vartheta, -\varphi) E'_{\varphi_V}(\vartheta, -\varphi) - E'_{\vartheta_V}(\vartheta, -\varphi) E'_{\varphi_H}(\vartheta, -\varphi)$ and

$$I_{V,H} = A \cos \vartheta e^{j\beta d \cos \vartheta} \int_{-\infty}^{+\infty} \int_{-\infty}^{+\infty} V_{V,H}(x, y) e^{j\beta x \sin \vartheta \cos \varphi} e^{j\beta y \sin \vartheta \sin \varphi} dx dy \quad (16)$$

A being a constant. Namely, the antenna far field is related to: i) the Fourier transforms I_V and I_H of the output voltages V_V and V_H of the probe for two independent sets of measurements (the probe is rotated by 90° in the second set); ii) the FF components E'_{ϑ_V} , E'_{φ_V} and E'_{ϑ_H} , E'_{φ_H} radiated by the probe and the rotated probe.

The values of V_V and V_H in the plane-rectangular grid needed to perform the described NF–FF transformation can be recovered from the bi-polar data via the OSI formula 10. Eq. 15 is valid whenever the probe maintains its orientation with respect to the AUT and this requires its co-rotation with the AUT. Probes exhibiting only a first-order azimuthal dependence in their radiated far field (such as an open-ended cylindrical waveguide excited by a TE_{11} mode) can be used without co-rotation, since V_V and V_H can be evaluated from the measured voltages V_φ and V_ρ , through the relations $V_V = V_\varphi \cos \varphi - V_\rho \sin \varphi$ and $V_H = V_\varphi \sin \varphi + V_\rho \cos \varphi$.

In the following we show some numerical tests relevant to a 3D-array of elementary Huygens sources linearly polarized along y and spaced 0.6λ along the radial and azimuthal lines and 2λ along z (λ being the wavelength). Only 7% of them, symmetrically placed and excited with respect to the plane $y=0$, are active. The excitation phases are the superposition of a random term, uniformly distributed in $[-\pi/2, \pi/2]$, and of a cubic x -dependent one. The amplitudes are tapered with respect to the x and y axes with a \cos^2 law. Such a source can be very well fitted by the proposed modelling with $a = 16\lambda$, $c = 5\lambda$ and $c' = 3\lambda$. The distance d is 10λ , and the bi-polar facility is characterized by $\delta_{\max} \approx 52.5^\circ$ and $L = 70\lambda$, so that the NF data lie in a circular zone of radius $\approx 62\lambda$. An open-ended cylindrical waveguide with radius 0.338λ is chosen as probe. Fig. 3 shows the reconstruction of the voltage V_V (the most significant one) on the radial line at $\varphi = 90^\circ$. As it can be seen, the

recovery is very accurate. To assess in a more quantitative way the algorithm performances, the maximum and mean-square reconstruction errors (normalized to the voltage maximum value on the plane) have been evaluated for $\chi = \chi' = 1.20$ and reported in Fig. 4. The algorithm stability has been tested by adding random errors to the exact samples in order to simulate a background noise (bounded to Δa in amplitude and with arbitrary phase) and an uncertainty on the data of $\pm\Delta a_r$ in amplitude and $\pm\Delta\phi$ in phase. As shown in Fig. 5, the algorithm is stable. The proposed OSI algorithm has been applied to efficiently recover the data required by the NF-FF transformation with plane-rectangular scanning. The corresponding E-plane pattern, reconstructed from the recovered plane-rectangular data lying in a $80\lambda \times 80\lambda$ square grid, is shown in Fig. 6. As can be seen, the FF reconstruction is very accurate also in the far out side lobes region, thus assessing the effectiveness of the technique. It may be interesting to compare the number of data (8 145) needed by the proposed technique with that (53 836) required by the standard bi-polar scanning technique [1] to cover the same scanning zone.

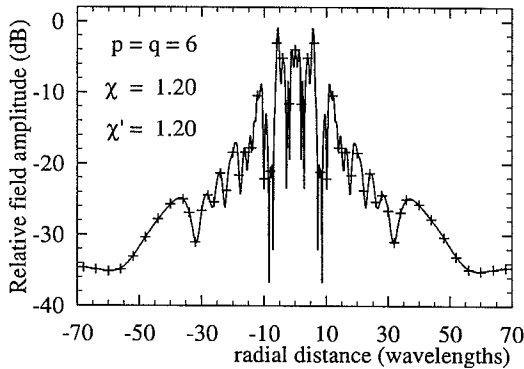


Fig.3 - Amplitude of the probe output voltage V_V on the radial line at $\phi = 90^\circ$. Solid line: exact. Crosses: interpolated.

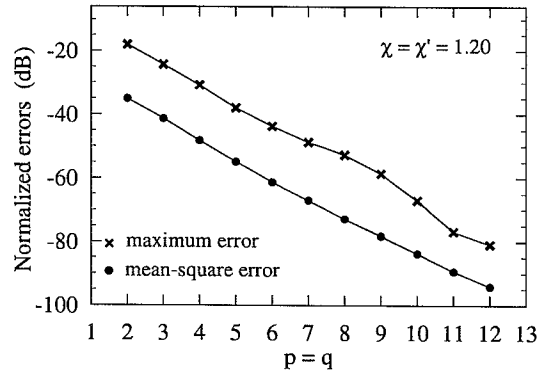


Fig.4 - Normalized reconstruction errors.

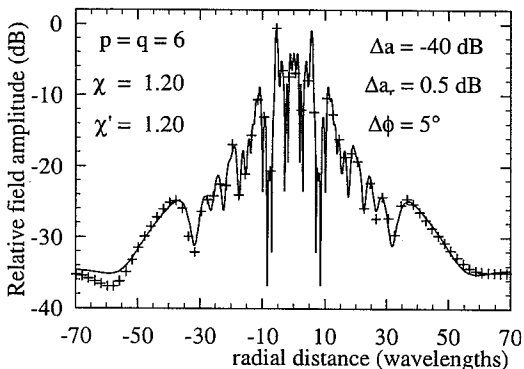


Fig.5 - Amplitude of the probe output voltage V_V on the radial line at $\phi = 90^\circ$. Solid line: exact. Crosses: interpolated from error affected data.

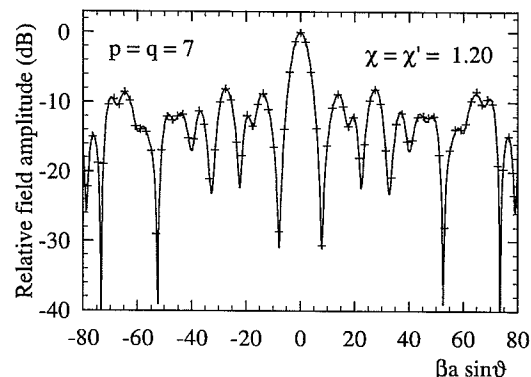


Fig.6 - FF pattern in the E-plane. Solid line: exact field. Crosses: reconstructed from probe-compensated bi-polar NF measurements.

REFERENCES

- [1] R.G.Yaccarino, Y.Rahmat-Samii, L.I.Williams, "The bi-polar near-field measurement technique, Part II: NF to FF transformation and holographic methods," *IEEE Trans. Antennas Prop.*, Vol.42, pp.196-204, 1994.
- [2] F.D'Agostino, C.Gennarelli, G.Riccio, C.Savarese, "Data reduction in the NF-FF transformation with bi-polar scanning," *Microw. Opt. Tech. Lett.*, Vol. 36, pp. 32-36, 2003.
- [3] O.M.Bucci, F.D'Agostino, C.Gennarelli, G.Riccio, C.Savarese, "NF-FF transformation with plane-polar scanning: ellipsoidal modelling of the antenna," *Automatika*, vol. 41, pp. 159-164, 2000.
- [4] O.M.Bucci, C.Gennarelli, C.Savarese, "Representation of electromagnetic fields over arbitrary surfaces by a finite and non redundant number of samples," *IEEE Trans. Antennas Prop.*, Vol.46, pp.351-359, 1998.
- [5] D.T.Paris, W.M.Leach, Jr., E.B.Joy, "Basic theory of probe-compensated near-field measurements," *IEEE Trans. Antennas Prop.*, Vol. AP-26, pp. 373-379, 1978.